Journal of Chromatography A, 1225 (2012) 70–78

Contents lists available at SciVerse ScienceDirect

Journal of Chromatography A

journal homepage: www.elsevier.com/locate/chroma

Effects of resin ligand density on yield and impurity clearance in preparative cation exchange chromatography. II. Process characterization

Jace Fogle*, Josefine Persson

Genentech Pharma Technical Development, 1 DNA Way MS 75A, South San Francisco, CA 94080, USA

ARTICLE INFO

Article history:
Received 15 July 2011
Received in revised form 2 November 2011
Accepted 15 December 2011
Available online 23 December 2011

Keywords:
Cation exchange chromatography
Monoclonal antibodies
Ligand density
SP Sepharose™ Fast Flow
Design of experiments
High-throughput screening

ABSTRACT

Ion exchange resins are key raw materials in biopharmaceutical manufacturing processes, and variability in ligand density has the potential to compromise process robustness if not controlled within appropriate ranges. In this study, yield and impurity clearance were evaluated for several preparative cation exchange chromatography steps using SP Sepharose™ Fast Flow resins at the high, low, and center of the commercial ligand density specification range. This was accomplished using a design of experiments (DoE) approach coupled to high-throughput screening in 96-well plate format, as well as column chromatography experiments with gradient elution. Results of the DoE study indicated that ligand density variation within the commercial specification range of SP Sepharose™ Fast Flow had no effect on yield, HCP clearance, aggregate clearance, or distribution of charge variants. However, results from the column experiments showed that ligand density has the potential to influence protein elution profiles which can lead to small changes in impurity clearance in some cases.

1. Introduction

Resin ligand density can influence both protein retention [1] and mass transfer [1–5] in cation exchange chromatography. In certain instances, these changes may affect impurity clearance [6]. This can be an important consideration during purification process development for biopharmaceutical products and other high value proteins. While resin manufacturers can diversify the selection of commercial ion exchangers available to end users by varying characteristics such as bead size and ligand density, lot-to-lot variation in raw materials such as chromatography resins has the potential to compromise process robustness. Since biopharmaceutical products must meet strict standards for consistency and quality, understanding the effects of raw material variability on purification process performance is a key aspect of qualification and validation activities. As Quality by Design [7] principles become an integral part of late-stage biopharmaceutical development, there is bound to be heightened interest in the effects of raw material variability in preparative chromatography processes. For example, ligand density variation in a commercial anion exchanger has already been implicated in yield losses during an intermediate wash step [8]. While the aforementioned study illustrates the importance of controlling resin properties in preparative ion exchange chromatography, it is an isolated case. The effects of resin ligand density on chromatography process robustness need to be studied in a more systematic manner.

The robustness of a biochemical processing step with respect to variations in specific input variables, and the potential for interactions between those variables, can be characterized using multivariate statistical analysis commonly referred to as "design of experiments" (DoE). This approach has already been applied successfully to industrial scale chromatographic purification steps [9,10]. These studies focused on affinity chromatography and hydrophobic interaction chromatography, respectively. Since statistical analytical approaches assume no insight into the biophysical mechanisms that actually drive process performance, large data sets are usually required to adequately capture significant responses to changes in the input variables.

Recently, process developers have been turning to high-throughput screening (HTS) methods using robotic liquid handling technology to expedite chromatography screening and modeling work [11–14]. It has been shown that results from batch-binding experiments in 96-well plate format can be very representative of data generated using chromatography columns at larger scale [11]. Moreover, HTS methods allow testing of many conditions in parallel, often with lower sample requirements. In this way, HTS approaches can facilitate more comprehensive process characterization studies in light of time or resource constraints.

The objective of this work was to use high-throughput screening and a design of experiments approach to directly evaluate the effects of ligand density variation on preparative cation exchange chromatography performance. This was accomplished using three

* Corresponding author. Tel.: +1 650 467 8417; fax: +1 650 225 4049.
E-mail address: persson.josefine@gene.com (J. Fogle).

0021-9673/$ – see front matter © 2011 Elsevier B.V. All rights reserved.
doi:10.1016/j.chroma.2011.12.049

Table 1
Monoclonal antibody feedstock.

Property	mAb B	mAb C	mAb X	mAb Y	mAb Z
Framework	IgG1	IgG1	IgG1	IgG1	IgG1
Theoretical p*I*	8.9	8.5	9.0	8.5	8.6
pH of cation exchange load	5.5	5.5	5.3	5.5	5.0
Conductivity of cation exchange load (mS/cm)	4.0	4.1	4.0	4.2	3.9
HMW species in Protein A pool (%)	11	<1	<1	<1	<1
Approximate HCP in Protein A pool (ng/mg[a])	8000	40,000	2000	2000	1000

[a] ng HCP/mg antibody.

prototypes of SP Sepharose™ Fast Flow, synthesized for this study, with ligand densities at the high, low, and center of the commercially available range. In addition, the results of this process characterization exercise were validated with a set of lab scale column chromatography experiments. In all cases, the resins were operated in bind-and-elute mode at conditions relevant to large scale biochemical manufacturing processes.

2. Materials and methods

2.1. Resins and columns

Experiments were performed on SP Sepharose™ Fast Flow (SPSFF). Three lots of SPSFF with the following ligand densities were used: 180 mequiv./L ("low" ligand density), 210 mequiv./L ("center point" ligand density), and 250 mequiv./L ("high ligand density"). These lots of resin were manufactured specifically for this study and provided by GE Healthcare Bio-Sciences (Uppsala, Sweden). This range of ligand densities corresponds to the commercial specification.

All resins were packed into 0.66 cm i.d. × 20 cm Omnifit columns (Bio-Chem Valve, Inc., Cambridge, England). All column chromatography experiments were performed on an ÄKTA™ Explorer 100 FPLC system with a 2 mm pathlength UV cell.

2.2. Feedstock

Full-length monoclonal antibodies (mAbs) were expressed in Chinese hamster ovary (CHO) cells in 2000 or 12,000 l bioreactors at Genentech (South San Francisco, Vacaville, or Oceanside, CA). Cell culture fluid was harvested using a combination of continuous centrifugation and depth filtration. Harvested cell culture fluid was initially purified using Protein A affinity chromatography with low pH elution. Protein A eluate was adjusted to pH 5.0–5.5 with 1.5 M Tris base and sterile filtered prior to use.

Table 1 lists the antibodies used in this work. mAbs X, Y, and Z were used in the HTS DoE study. These three antibodies have typical impurity profiles with less than 1% high molecular weight variants in the cation exchange load. Further, these mAbs have well-established step elution conditions on SP Sepharose™ Fast Flow. mAbs B and C were used for the column experiments. The mAb B cation exchange load comprised approximately 11% aggregate by mass. mAb C had nearly undetectable levels of high molecular weight variants, but the cation exchange load had relatively high levels of host cell protein (HCP) impurities (approximately 10-fold higher than other mAbs employed in this study).

2.3. High performance size exclusion chromatography (HPLC-SEC)

An HPLC-SEC assay was used to quantify the amount of aggregate in the cation exchange load and elution fractions. The assay used a TSK G3000SWXL (7.8 × 300 mm) column (cat. No. 08541) from Tosoh Bioscience (Montgomeryville, PA). The column was run at 0.5 mL/min for 30 min in 0.20 M potassium phosphate, 0.25 M potassium chloride, pH 6.2. The column was run at ambient temperature and monitored at 280 nm. The target mass for each injection was 50 μg. Additional details on this assay can be found in previous work [6].

2.4. Dynamic binding capacity experiments

The resin dynamic binding capacities at 1% breakthrough ($DBC_{1\%}$) were measured at 150 cm/h (8 min residence time). For purposes of this study, 1% breakthrough was defined as the column load density (grams of antibody loaded per liter of packed bed) at which antibody concentration in the column effluent was equal to one percent of the antibody concentration in the load.

Column effluent was collected in 2 mL fractions, and the concentration of antibody in the fractions was quantified by UV absorbance at 279 nm.

2.5. Column chromatography—assessing HMW and HCP clearance

The cation exchange columns were initially equilibrated with five column volumes (CV) of 50 mM sodium acetate, pH 5.5. mAbs B and C (adjusted to approximately pH 5.5 and 4 mS/cm as described in Section 2.2) were then loaded to 80% of $DBC_{1\%}$. The columns were washed with five CV of 50 mM sodium acetate, pH 5.5. Antibody was eluted with a 10–90% gradient in 15 CV. Buffer A was 50 mM sodium acetate, pH 5.5. Buffer B was 500 mM sodium acetate, pH 5.5 for mAb B and 350 mM sodium acetate, pH 5.5 for mAb C.

For mAb B, the elution pool was collected in 2 mL fractions for assessing aggregate clearance. Elution fractions were analyzed using HPLC-SEC (see Section 2.3). The percent of HMW impurity present in the cumulative end product pool (%HMW) was calculated as follows:

$$\%\mathrm{HMW} = \frac{\sum_{i=1}^{n}(C_i \ \ [\mathrm{mg/mL}])(\mathrm{HPLC}_i)}{\sum_{i=1}^{n}(C_i \ \ [\mathrm{mg/mL}])} \times 100 \quad (1)$$

where C_i is the mAb concentration in fraction i, HPLC_i is the mass fraction of HMW species present in fraction i, and n is the number of fractions collected at any point during elution.

For mAbs B and C, the elution pool was fractionated according to optical density (OD) at the outlet of the column for assessing HCP clearance. Fractions corresponding to 0.5–2.0 OD, 2.0–1.0 OD, and 1.0–0.5 OD were collected. HCP in the elution pools was quantified using an ELISA that was developed at Genentech in well plate format.

2.6. Design of experiments (DoE)

Four input variables, or factors, were examined in this study: resin ligand density, protein load density, elution buffer pH, and elution buffer conductivity. The characterization range for each of these factors was marginally wider than the acceptable operating limits for the cation exchange step at scale; Table 2 lists the high, low, and center point values used for each factor. The process responses included in this study were yield, aggregate, HCP, and distribution of charged variants in the elution pool. The study design was a full factorial with four center points.

In addition, a small univariate study was conducted with resin ligand density as the sole factor. Operating conditions for these runs were identical to the DoE except that only ligand density was changed; four replicates were performed with each mAb at each ligand density. Tables 3 and 4 list the experiments performed for the DoE and the univariate study, respectively.

Table 2
SP Sepharose™ Fast Flow characterization study design.

mAb	Factor	Low	Center	High
X	Equil and wash buffer	25 mM HEPES pH 7.0		
	Resin ligand density (mequiv./L)	180	210	250
	mAb load density (mg/mL bed volume)	20	35	50
	Elution buffer pH	6.7	7.0	7.3
	Elution buffer conductivity (mS/cm)	6.0	6.8	7.5
Y	Equil and wash buffer	50 mM acetate pH 5.5		
	Resin ligand density (mequiv./L)	180	210	250
	mAb load density (mg/mL bed volume)	10	25	40
	Elution buffer pH	5.2	5.5	5.8
	Elution buffer conductivity (mS/cm)	9.5	10.5	12.0
Z	Equil and wash buffer	25 mM HEPES pH 8.0		
	Resin ligand density (mequiv./L)	180	210	250
	mAb load density (mg/mL bed volume)	10	25	40
	Elution buffer pH	7.9	8.0	8.1
	Elution buffer conductivity (mS/cm)	3.1	3.3	3.6

Table 3
SP Sepharose™ Fast Flow characterization study experiments.

Run no.	Ligand density	Load density	pH	Conductivity
1	Low	Low	Low	Low
2	Low	Low	Low	High
3	Low	Low	High	Low
4	Low	Low	High	High
5	Low	High	Low	Low
6	Low	High	Low	High
7	Low	High	High	Low
8	Low	High	High	High
9	High	Low	Low	Low
10	High	Low	Low	High
11	High	Low	High	Low
12	High	Low	High	High
13	High	High	Low	Low
14	High	High	Low	High
15	High	High	High	Low
16	High	High	High	High
17	Center	Center	Center	Center
18	Center	Center	Center	Center
19	Center	Center	Center	Center
20	Center	Center	Center	Center

Data was analyzed using JMP® software (SAS Institute, Cary, NC). For purposes of this work, the effects of individual factors and interactions between factors on process responses were considered statistically significant when the p value was less than 0.05. (The p value refers to the probability that random testing of two populations of identical samples would result in mean responses with a difference greater than that observed in the actual experiment.)

96-Well PreDictor™ plates were prepared using three lots of SP Sepharose™ Fast Flow (described in Section 2.1) at GE Healthcare Bio-Sciences (Uppsala, Sweden). Resin slurry equivalent to 50 μL settled bed volume was added to each well. The 96-well plates were run on a TECAN Freedom Evo 200 (Tecan US, Research Triangle Park, NC) liquid handling system at Genentech (South San Francisco, CA). The 96-well plates were centrifuged at 1200 × g for 3 min to separate resin from supernatant. Protein concentrations in the supernatants were measured using UV absorbance at 280 nm on the TECAN system.

Table 4
SP Sepharose™ Fast Flow characterization study experiments (univariate study).

Run no.	Ligand density	Load density	pH	Conductivity
1	Low	Center	Center	Center
2	Low	Center	Center	Center
3	Low	Center	Center	Center
4	Low	Center	Center	Center
5	High	Center	Center	Center
6	High	Center	Center	Center
7	High	Center	Center	Center
8	High	Center	Center	Center
9	Center	Center	Center	Center
10	Center	Center	Center	Center
11	Center	Center	Center	Center
12	Center	Center	Center	Center

All operations were performed in an automated fashion using the TECAN liquid handling system. The resins were equilibrated with three successive cycles of buffer addition, plate agitation, and plate centrifugation. The plates were agitated for 80 min after loading protein to allow sufficient time for intraparticle diffusion and adsorption. Next, two wash cycles were performed with equilibration buffer to remove unbound protein. A total of five elution cycles were performed, and the first four elution pools were combined for further analysis. Finally, the resin was stripped with two cycles of 1 M sodium chloride. All buffer and sample additions were 300 μL.

3. Results and discussion

3.1. High-throughput screening results

Results of the DoE indicate that resin ligand density does not affect process performance within the ranges tested here. The scatter plots in Fig. 1 were generated in JMP® and provide a convenient summary of all the data collected in this study. None of the process responses appear to be strongly correlated with ligand density for any of the mAbs upon visual inspection of the data. Statistical analysis by JMP® supports this conclusion; the p values corresponding to all of the model parameters for ligand density and for interactions of ligand density with other factors are greater than 0.05. This is illustrated in Fig. 2A for mAb Y yield; only the factors with p values less than 0.05 are statistically significant (indicated by the vertical blue lines in the histogram). Here three significant effects were found: both elution buffer pH and conductivity strongly influenced mAb Y yield, and there was an interaction between pH and conductivity. The negative model parameter associated with this interaction is an example of interference—the combined effect of changing elution buffer pH and conductivity is less than the additive effect of changes in the individual factors. Fig. 2B shows another example of JMP® output for mAb Z aggregate clearance. In this case protein load density is the only process variable that has a statistically significant effect on the response. This is an interesting example in the sense that load density has a statistically significant effect on aggregate clearance and this effect is clear from inspection of the raw data; however, this effect might not be considered "practically significant" since the absolute changes in aggregate level in the elution pools are very small and well below the acceptable limit for a therapeutic mAb preparation. Table 5 summarizes all of the statistically significant factors and interactions for mAb X, mAb Y, and mAb Z found in this study. Clearly multivariate statistical analysis cannot provide insight into the biophysical mechanisms that control process performance; further, the results of statistical analyses such as this one must be interpreted in light of final product quality specifications and operational constraints. However, HTS coupled to multivariate statistical analysis can be an effective approach for measuring the relative significance of numerous process variables across their acceptable operating ranges and beyond. In this case, the results are important because they demonstrate that the experimental design employed here was capable of identifying statistically significant factors and interactions, yet ligand density was not implicated as one of those factors.

The results of the univariate study (with ligand density as the only variable) are completely consistent with the DoE study. No trend in yield, aggregate, HCP, or cIEF main peak area was observed for any of the mAbs (Fig. 3) over the range 180–250 mequiv./L. These

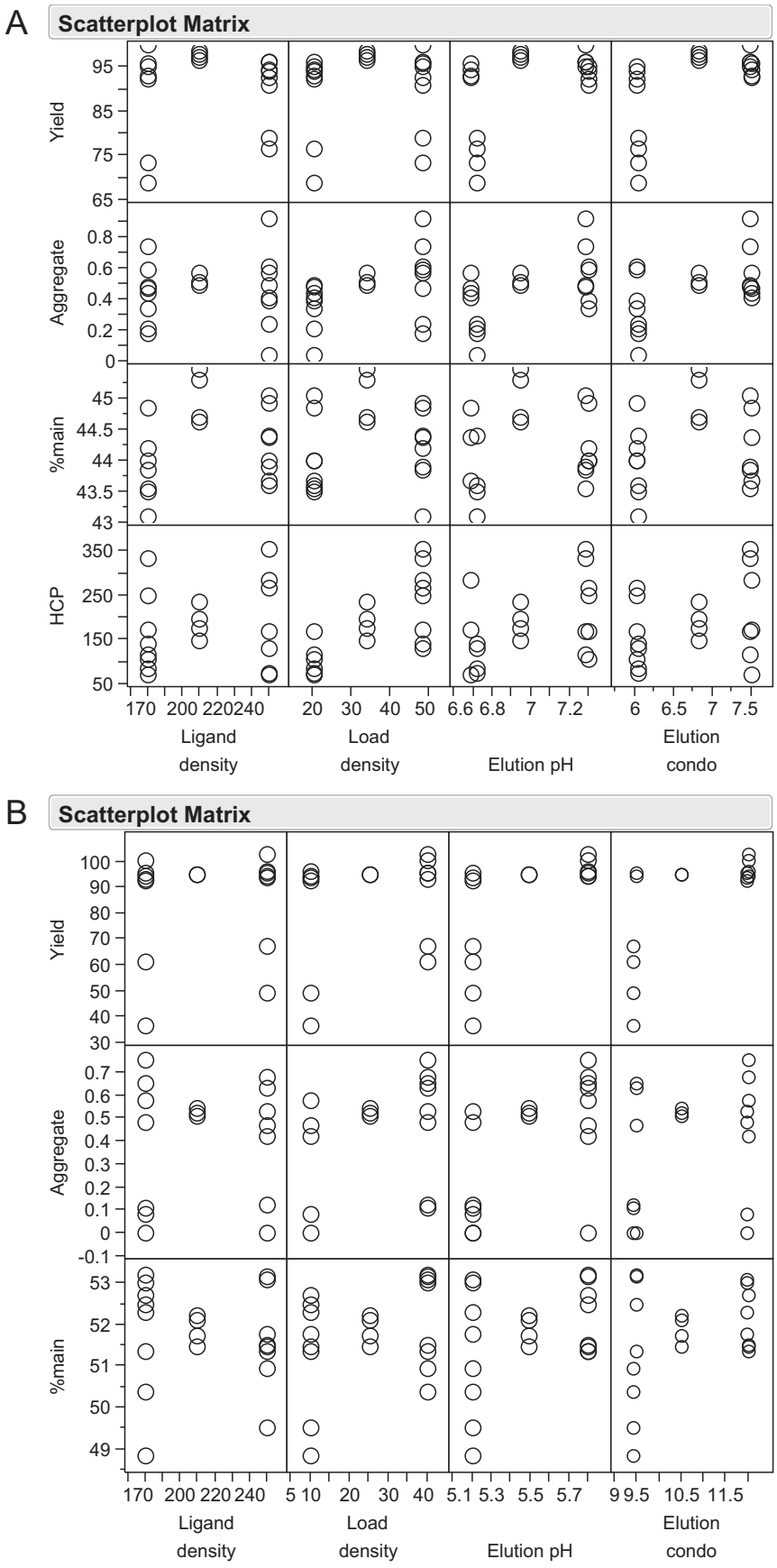

Fig. 1. Scatterplots generated in JMP® for the DoE process characterization study. (A) mAb X, (B) mAb Y, (C) mAb Z.

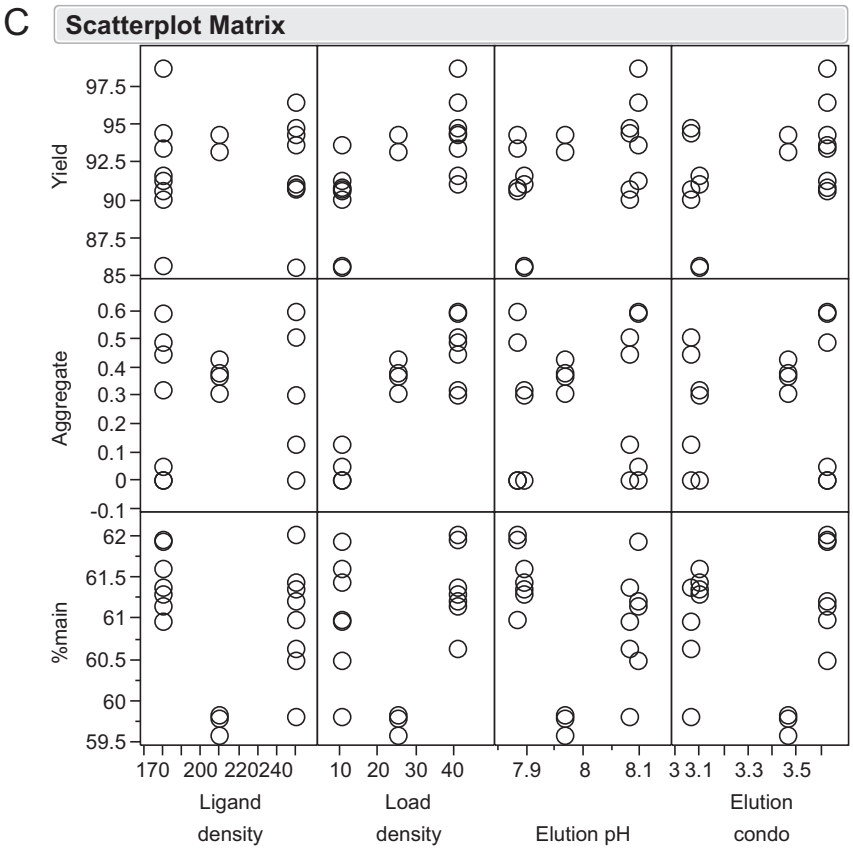

Fig. 1. (*Continued*).

results are also consistent with work performed using a set of prototype cation exchangers which spanned a wider ligand density range (45–154 mequiv./L) [6]. In that case, ligand density was found to have no effect on yield or aggregate clearance, and distribution of charge variants was unchanged with the exception of one basic variant present in unusually high quantities in one of the mAb feedstocks. While there was an effect on HCP clearance for one mAb at very low ligand densities in the previous study, the levels of HCP in the cation exchange load materials used here were much more representative of typical Protein A elution pools.

Table 5
SP Sepharose™ Fast Flow characterization study results.

mAb	Response	Significant factors and interactions	Effect size
X	Yield	Elution buffer conductivity	6.36
	HCP[a]	Load density	66.17
		Elution buffer pH	46.84
	Aggregate	Elution buffer conductivity	0.13
		Elution buffer pH	0.13
		mAb load density	0.09
	cIEF main peak area		
Y	Yield	Elution buffer pH	11.48
		Elution buffer conductivity	10.61
		Elution buffer pH × elution buffer conductivity	−9.45
	Aggregate	Elution buffer pH	0.18
		mAb load density	0.15
	cIEF main peak area	Elution buffer pH × elution buffer conductivity	−0.88
		Elution buffer pH	0.47
		Elution buffer conductivity	0.46
		mAb load density	0.40
		mAb load density × elution buffer conductivity	−0.31
Z	Yield	mAb load density	2.29
		Elution buffer pH	1.88
		Elution buffer conductivity	1.76
	Aggregate	mAb load density	0.23
	cIEF main peak area		

[a] HCP was below assay detection limits in mAb Y and mAb Z elution pools.

Packed bed chromatography results

The last portion of this work was aimed at verifying the results of the DoE study in column format with antibody feedstocks containing high levels of impurities relative to those used for the batch binding experiments. mAbs B and C were selected for this purpose, as they have typical distributions of charge variants but unusually high amounts of aggregate and host cell protein, respectively. The resins were loaded to 80% of their $DBC_{1\%}$ to compensate for any differences in binding capacity and to test the resins at conditions representative of large scale manufacturing processes. These experiments were intended to provide a "worst case" scenario for elucidating any changes in process performance that might arise as a result of ligand density variation within the specification range of a commercially available resin.

SPSFF dynamic binding capacity for both mAb B and C decreased with increasing ligand density in the range 180–250 mequiv./L. Fig. 4 shows that the decrease in $DBC_{1\%}$ across the entire ligand density range is approximately 10% for both mAbs. This effect is very likely due to charge-induced steric exclusion on the resin surface [15] and is consistent with the results of Hardin and co-workers [5]. This is in contrast with the results from a parallel study using prototype cation exchangers [6] where $DBC_{1\%}$ increased with ligand density, presumably due to changes in the retention of the antibodies on the resins. While the base matrices of the aforementioned

A

Sorted Parameter Estimates

Term	Estimate	Prob>|t|
Elution pH(5.2,5.799)	11.480782	0.0135*
Elution condo(9.43,12)	10.610794	0.0182*
Elution pH*Elution condo	-9.447546	0.0272*
Load density(10.056,40.254)	3.7553149	0.2374
Load density*Elution pH*Elution condo	3.2160265	0.3109
Load density*Elution condo	-1.878514	0.5333
Load density*Elution pH	-1.832036	0.5378
Ligand density*Elution pH*Elution condo	1.3422813	0.6539
Ligand density(180,250)	1.2373684	0.6705
Ligand density*Elution pH	-1.070775	0.7141
Ligand density*Elution condo	-0.611567	0.8354
Ligand density*Load density*Elution condo	0.4995829	0.8651
Ligand density*Load density*Elution pH*Elution condo	-0.487599	0.8690
Ligand density*Load density*Elution pH	0.3523769	0.9032
Ligand density*Load density	-0.284684	0.9213

B

Sorted Parameter Estimates

Term	Estimate	Prob>|t|
Load density(10.188,40.92)	0.2275692	0.0013*
Elution condo(3.06,3.62)	0.0499304	0.1576
Load density*Elution condo	0.0504836	0.1592
Elution pH(7.884,8.097)	0.0403084	0.2533
Elution pH*Elution condo	-0.02848	0.4151
Ligand density*Elution pH*Elution condo	-0.02474	0.4744
Load density*Elution pH	0.0207752	0.5314
Ligand density*Load density*Elution condo	0.0169462	0.5931
Load density*Elution pH*Elution condo	-0.014374	0.6706
Ligand density(180,250)	0.0115165	0.7032
Ligand density*Elution condo	-0.007321	0.8145
Ligand density*Elution pH	0.0069789	0.8295
Ligand density*Load density*Elution pH	-0.006003	0.8529
Ligand density*Load density	0.0044034	0.8834
Ligand density*Load density*Elution pH*Elution condo	-0.000269	0.9936

Fig. 2. Pareto plot and corresponding model parameters generated in JMP® for (A) mAb Y yield, (B) mAb Z aggregate clearance. Vertical blue lines indicate $p < 0.05$. (For interpretation of the references to color in this figure legend, the reader is referred to the web version of the article.)

prototype resins and SPSFF are different, it seems that there may be a trade-off between increasing retention and decreasing transport into the resin pores as ligand density increases.

No significant differences in resolution of mAb B aggregate were observed across the ligand density range examined here. Fig. 5 shows cumulative aggregate in the product pool as a function of antibody yield; the curves for the 180 mequiv./L and 210 mequiv./L resins lie almost on top of one another while the curve for the 250 mequiv./L resin lies just below. This may indicate that aggregate clearance on the highest ligand density resin was marginally better than the other two, but the difference was less than one percent at all yields. Further, the total antibody yield on all three resins was very similar. These results are consistent with those obtained on the prototype cation exchangers discussed previously [6].

One interesting feature of the aggregate versus yield curves in Fig. 5 is that the early fractions contain varying amounts of aggregate. This effect was not observed in the other study [6]. In particular, the first three fractions to elute from the 250 mequiv./L column were slightly enriched in aggregate relative to the 210 mequiv./L and 180 mequiv./L fractions. While it is possible that the early-eluting aggregate is structurally or chemically different than the late-eluting aggregate, this is not likely since no differences in the HPLC-SEC chromatograms were observed under any condition. Moreover, a small leading edge shoulder was observed on the 250 mequiv./L elution peak, and the position of this shoulder coincided closely with the early-eluting aggregate (Fig. 6). Upon closer inspection, small differences in the pH and conductivity profiles were also noted at the beginning of the salt gradient where buffer B concentration was increased in stepwise fashion from zero to 10 percent (Figs. 7 and 8). Step changes in mobile phase salt concentration have been shown to cause transient changes in mobile phase pH in ion exchange chromatography [16–18]; further, the magnitude of transient pH and conductivity changes is related to the inherent buffering capacity of the ion exchange resin and can be affected by ligand density [19]. Here, it seems that increased ligand density leads to temporary shallowing of the conductivity profile immediately after the step change in buffer B. These changes are very small, but apparently they are large enough to affect the front end of the antibody elution profile.

The leading edge shoulder was also observed on the mAb C elution profile at 250 mequiv./L (Fig. 9). Since the mAb C feedstock did not contain detectable aggregate, it is unlikely that either the mAb B or the mAb C shoulder was caused by the early elution of aggregate. Rather, the shouldering must be a direct result of the pH transition occurring around 2 CV (column volumes after gradient is initiated), and the appearance of mAb B aggregate in early elution fractions must be an unrelated effect possibly resulting from differences in retention and/or mass transfer rates of the monomer and aggregate on the 250 mequiv./L resin. The differences in antibody elution profile observed here would not have been elucidated using batch binding experiments.

It also appears that HCP clearance was influenced by resin ligand density in this set of column experiments. HCP was removed more effectively at higher ligand densities for both mAb B and C, although this is clearer in the case of mAb C. Fig. 10 shows the HCP levels in the product pools for three different end-pool criteria (optical density, OD, of 2.0, 1.0, or 0.5). Trends in HCP clearance with ligand density are most obvious for the narrowest elution pools (pooling

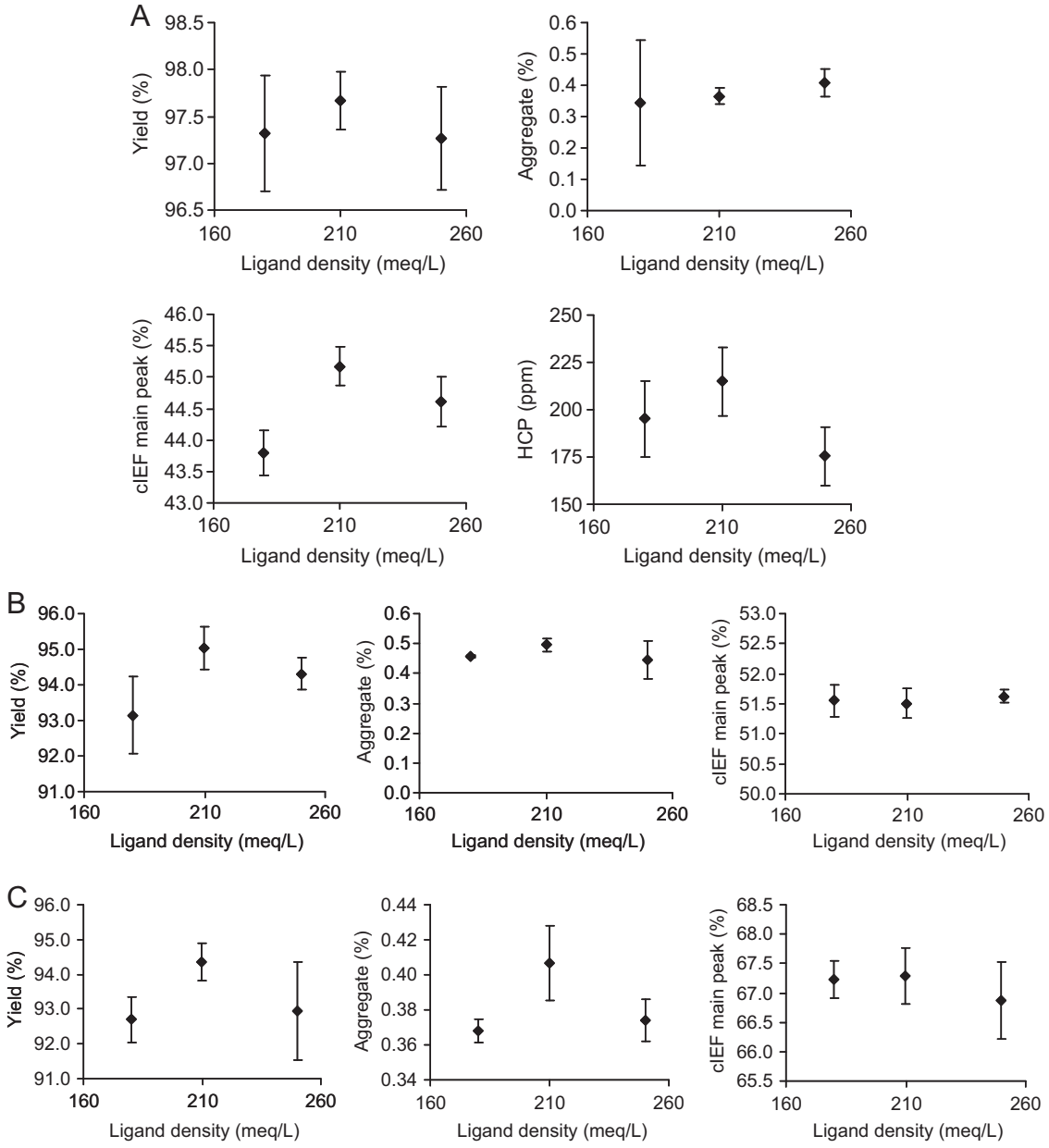

Fig. 3. Univariate process characterization study results. (A) mAb X, (B) mAb Y, (C) mAb Z. Magnitude of the error bars is one standard deviation from the mean.

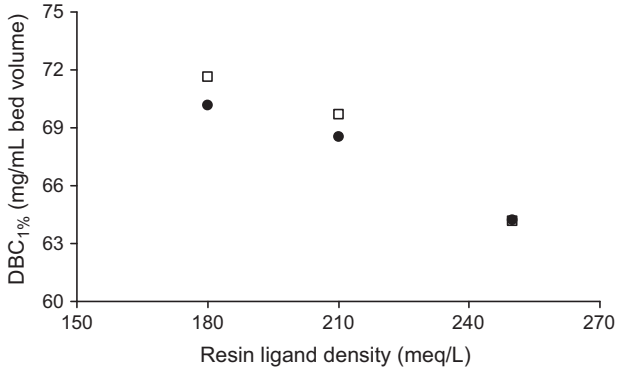

Fig. 4. mAb dynamic binding capacities at 1% breakthrough ($DBC_{1\%}$) on SP Sepharose™ Fast Flow. (□) mAb B, (●) mAb C.

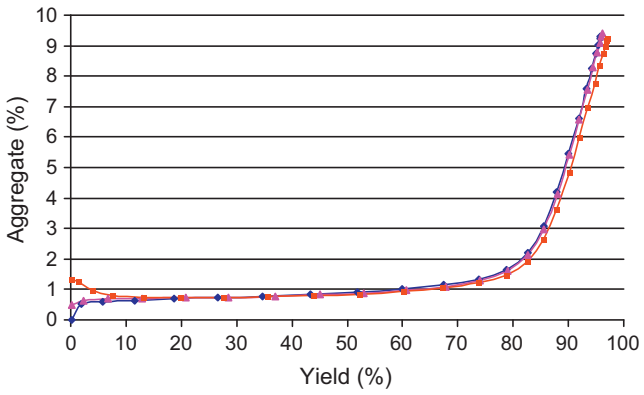

Fig. 5. Aggregate versus total antibody yield for mAb B on SP Sepharose™ Fast Flow at 80% of $DBC_{1\%}$. (♦) 180 mequiv./L, (▲) 210 mequiv./L, (■) 250 mequiv./L. Lines between the data points are for visual purposes only.

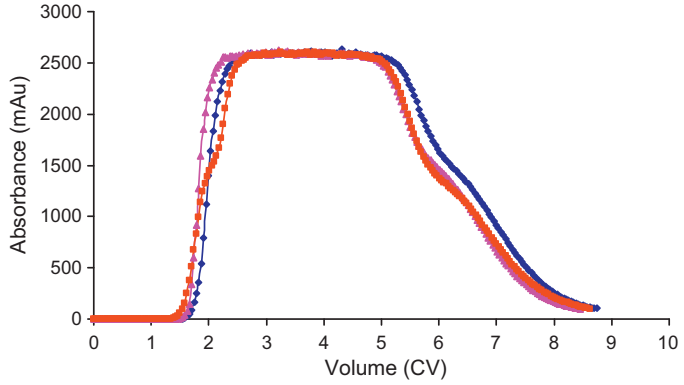

Fig. 6. mAb B elution curves on SP Sepharose™ Fast Flow at 80% of $DBC_{1\%}$. (♦) 180 mequiv./L, (▲) 210 mequiv./L, (■) 250 mequiv./L.

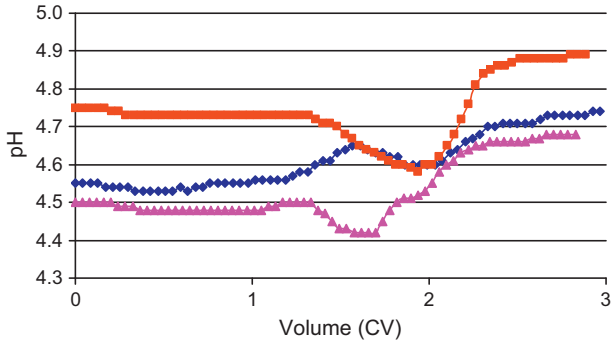

Fig. 7. mAb B pH profiles on SP Sepharose™ Fast Flow at 80% of $DBC_{1\%}$. (♦) 180 mequiv./L, (▲) 210 mequiv./L, (■) 250 mequiv./L.

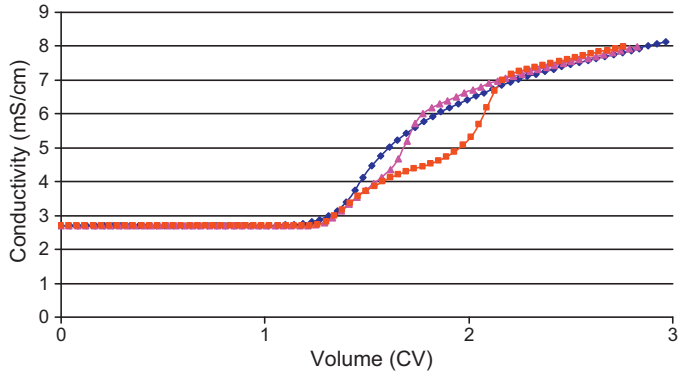

Fig. 8. mAb B conductivity profiles on SP Sepharose™ Fast Flow at 80% of $DBC_{1\%}$. (♦) 180 mequiv./L, (▲) 210 mequiv./L, (■) 250 mequiv./L.

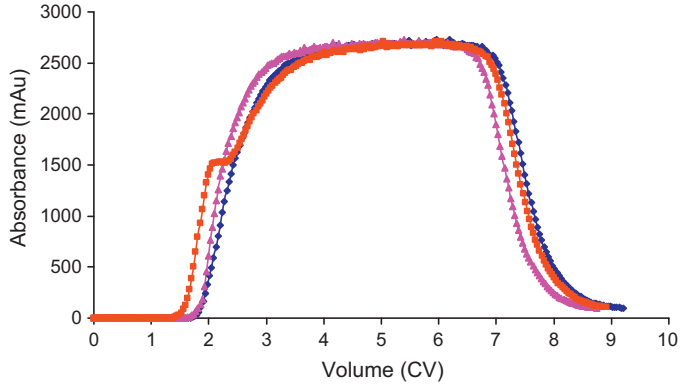

Fig. 9. mAb C elution curves on SP Sepharose™ Fast Flow at 80% of $DBC_{1\%}$. (♦) 180 mequiv./L, (▲) 210 mequiv./L, (■) 250 mequiv./L.

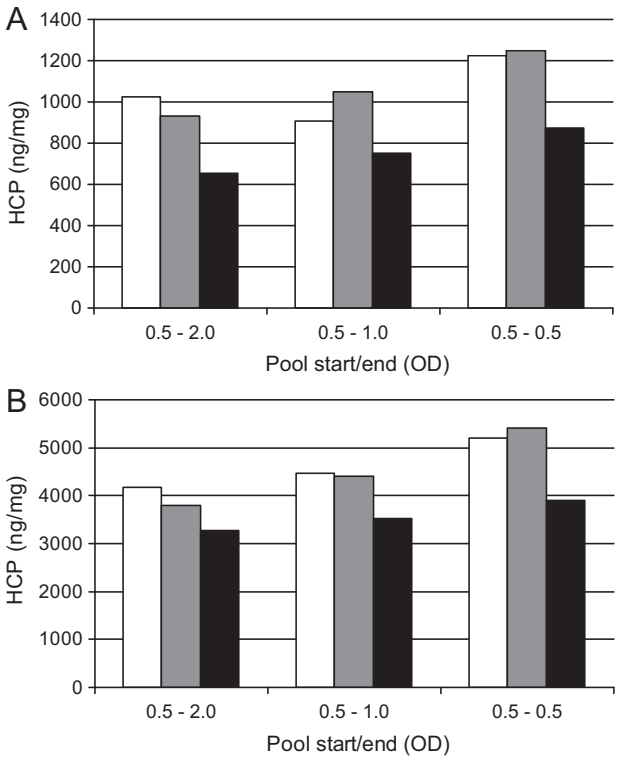

Fig. 10. Host cell protein levels in SP Sepharose™ Fast Flow product pools following loading to 80% of $DBC_{1\%}$. Yields were between 92 and 100% for all elution pools. (A) mAb B, (B) mAb C. Resins: (□) 180 mequiv./L, (■) 210 mequiv./L, (■) 250 mequiv./L.

ended at 2.0 OD); this indicates that selectivity differences between the resins are greatest at low salt concentrations (early in the gradient). It is possible that these differences are caused by artificial shallowing of the beginning of the gradient (Fig. 8) rather than by real differences in retention between the mAb and the HCP species. This might explain why ligand density affected HCP clearance for mAbs B and C in the column experiments but not for mAb X in the batch binding experiments. However, it is also possible that the effect of ligand density on HCP clearance becomes more significant when there are higher levels of HCP in the load material. The initial concentration of HCP in the mAb B and C load material was several-fold higher than that for mAb X (see Table 1). It is also important to point out that the differences in HCP levels observed in these product pools were small. Here, cation exchange was used downstream of capture on Protein A; there is reason to believe that HCP would be cleared to undetectable levels in all cases after a second polishing step [20].

4. Conclusions

Cation exchange resin ligand density can affect process performance, but the nature and extent of those effects is highly dependent on feedstock and operating conditions. Here, we observed differences in the pH and conductivity profiles during a salt gradient elution step on a set of three SP Sepharose™ Fast Flow prototypes with a ligand density range of 180–250 mequiv./L. Specifically, the differences were observed at the beginning of the gradient following a step change in buffer B concentration from zero to 10 percent. While these differences were subtle, they appear to have influenced the protein elution profile, and they may also have affected HCP clearance. Overall yield and HMW variant clearance were not affected. These effects were not observed on a set of five prototype cation exchangers with a ligand density range of 45–154 mequiv./L [6]; this is consistent with the idea that they

were caused by intrinsic buffering capacity of the higher ligand density resins. In general, these results suggest that ligand density variation should be considered when developing and validating commercial cation exchange chromatography processes; however, tightening controls on acceptable ligand density ranges beyond the manufacturer specification may only be warranted in specific cases.

A multivariate DoE study performed using high throughput screening and three mAbs with typical impurity levels in the load materials did not reveal any effect of ligand density on impurity clearance within the ranges tested. However, pH and conductivity transitions likely would not have influenced these results because the 96-well plate experiments were performed under pseudo-equilibrium conditions. Clearly, conclusions regarding ligand density variation and its impact on process performance under one set of conditions should not be extended to other situations without careful consideration of the feedstock and experimental design.

Acknowledgements

The author would like to thank GE Healthcare Bio-Sciences (Uppsala, Sweden) for graciously providing samples of SP Sepharose™ Fast Flow prototypes.

The author would like to thank Paul McDonald for assistance with the TECAN liquid handling system.

References

[1] D. Wu, R.R. Walters, J. Chromatogr. 598 (1992) 7.
[2] J.F. Langford, X. Xu, Y. Yao, S.F. Maloney, A.M. Lenhoff, J. Chromatogr. A 1163 (2007) 190.
[3] A. Franke, N. Forrer, A. Butté, B. Cvijetić, M. Morbidelli, M. Jöhnck, M. Schulte, J. Chromatogr. A 1217 (2010) 2216.
[4] P. DePhillips, A.M. Lenhoff, J. Chromatogr. A 933 (2001) 57.
[5] A.M. Hardin, C. Harinarayan, G. Malmquist, A. Axén, R. van Reis, J. Chromatogr. A 1216 (2009) 4366.
[6] J. Fogle, N. Mohan, E. Cheung, J. Persson, J. Chromatogr A 1225 (2012) 62–69.
[7] Guidance for Industry Q8 Pharmaceutical Development, U.S. Department of Health and Human Service, Food and Drug Administration (FDA), 2006.
[8] D. Cecchini, Applications of Design Space for Biopharmaceutical Purification Processes, Quality by Design for Biopharmaceuticals, John Wiley & Sons, Inc., Hoboken, New Jersey, 2009, pp. 138–141.
[9] A.A. Shukla, L. Sorge, J. Boldman, S. Waugh, Biotechnol. Appl. Biochem. 34 (2001) 71.
[10] C. Jiang, L. Flansburg, S. Ghose, P. Jorjorian, A.A. Shukla, Biotechnol. Bioeng. 107 (2010) 985.
[11] J.L. Coffman, J.F. Kramarczyk, B.D. Kelley, Biotechnol. Bioeng. 100 (2008) 605.
[12] J.F. Kramarczyk, B.D. Kelley, J.L. Coffman, Biotechnol. Bioeng. 100 (2008) 707.
[13] D.L. Wensel, B.D. Kelley, J.L. Coffman, Biotechnol. Bioeng. 100 (2008) 839.
[14] B.D. Kelley, M. Switzer, P. Bastek, J.F. Kramarczyk, K. Molnar, T. Yu, J.L. Coffman, Biotechnol. Bioeng. 100 (2008) 950.
[15] C. Harinarayan, J. Mueller, A. Ljunglöf, R. Fahrner, J. Van Alstine, R. van Reis, Biotechnol. Bioeng. 95 (2006) 775.
[16] S. Ghose, T.M. McNerney, B. Hubbard, Biotechnol. Prog. 18 (2002) 530.
[17] T.M. Pabst, G. Carta, J. Chromatogr. A 1142 (2007) 19.
[18] T.M. Pabst, D. Antos, G. Carta, N. Ramasubramanyan, A.K. Hunter, J. Chromatogr. A 1181 (2008) 83.
[19] J. Fogle, J. Hsiung, J. Chromatogr. A 1217 (2010) 660.
[20] D.K. Follman, R.L. Fahrner, J. Chromatogr. A 1024 (2004) 79.